

Axitinib overcomes multiple imatinib resistant cKIT mutations including the gatekeeper mutation T670I in gastrointestinal stromal tumors

Feiyang Liu*, Fengming Zou*, Cheng Chen*, Kailin Yu*, Xiaochuan Liu, Shuang Qi, Jiaxin Wu, Chen Hu, Zhenquan Hu, Juan Liu, Xuesong Liu, Li Wang, Juan Ge, Wenchao Wang, Tao Ren, Mingfeng Bai, Yujiao Cai, Xudong Xiao, Feng Qian, Jun Tang, Qingsong Liu and Jing Liu 

Ther Adv Med Oncol

2019, Vol. 11: 1–15

DOI: 10.1177/
1758835919849757

© The Author(s), 2019.
Article reuse guidelines:
sagepub.com/journals-
permissions

Abstract

Background: cKIT kinase overexpression and gain-of-function mutations are the critical pathogenesis of gastrointestinal stromal tumors (GISTs). Although the multiple kinase inhibitors such as imatinib, sunitinib, and regorafenib have been approved for GISTs, the acquisition of polyclonal secondary resistance mutations in KIT is still a limitation for GIST treatment. Here we explored the KIT inhibitory activity of axitinib in preclinical models and describe initial characterization of its activity in GIST patient-derived primary cells.

Methods: The activities of axitinib against mutant KIT were evaluated using protein-based assay and a panel of engineered and GIST-derived cell lines. The binding modes of axitinib-KIT/KIT mutants were analyzed. Four primary cells derived from GIST patients were also used to assess the drug response of axitinib.

Results: Axitinib exhibited potent activities against a variety of cKIT associated primary and secondary mutations. It displayed better activity against cKIT wild-type, cKIT V559D/A/G, and L576P primary gain-of-function mutations than imatinib, sunitinib, and regorafenib. In addition, it could inhibit imatinib resistant cKIT T670I and V654A mutants *in vitro* and *in vivo* GIST preclinical models.

Conclusion: Our results provide the basis for extending the application of axitinib to GISTs patients who are unresponsive or intolerant to the current therapies.

Keywords: axitinib, cKIT, cKIT T670I, GISTs, drug resistance

Received: 6 October 2018; revised manuscript accepted: 4 April 2019.

Introduction

Gastrointestinal stromal tumors (GISTs) are the most common mesenchymal tumors of the gastrointestinal tract. Constitutive activation of cKIT kinase mediated signaling pathway is essential for the tumorigenesis of GISTs.^{1,2} cKIT kinase is a type III receptor tyrosine kinase that upon stem cell factor (SCF) stimulation will activate downstream signaling pathways such as RAS/RAF/ERK and PI3K/AKT to regulate the cell proliferation, survival, apoptosis, and differentiation. Approximately 75% GISTs harbor oncogenic

gain-of-function KIT gene mutations that mimic the SCF-induced constitutive signaling pathway activation.³ Currently, over 20 different functional mutations have been identified in the clinic.⁴ Most primary mutations such as L576P and V559D/A/G mutants occur in the extracellular domain and juxtamembrane (JM) domain.^{5–7} Secondary mutations are induced by drug treatment and usually located at the ATP binding pocket such as cKIT V654A and the gatekeeper mutant T670I, or at the activation loop such as D816V/H, N822K, and A829P.^{8–10}

Correspondence to:

Jing Liu
High Magnetic Field Laboratory, Chinese Academy of Sciences, 350 Shushanhu Road, Hefei, Anhui 230031, P. R. China Precision Medicine Research Laboratory of Anhui Province, Hefei, Anhui 230088, P. R. China
jingliu@hmf.ac.cn

Qingsong Liu
High Magnetic Field Laboratory, Chinese Academy of Sciences, 350 Shushanhu Road, Hefei, Anhui 230031, P. R. China Precision Medicine Research Laboratory of Anhui Province, Hefei, Anhui 230088, P. R. China University of Science and Technology of China, Hefei, Anhui 230036, P. R. China Precision Targeted Therapy Discovery Center, Institute of Technology Innovation, Hefei Institutes of Physical Science, Chinese Academy of Sciences, Hefei, Anhui 230088, P. R. China Institute of Physical Science and Information Technology, Anhui University, Hefei, Anhui 230601, P. R. China
qslu97@hmf.ac.cn

Jun Tang
Department of Gastroenterology, The People's Liberation Army Joint Logistics Support Force No. 901 Hospital, Hefei, Anhui 230031, P. R. China
tangjun1974@163.com

Feiyang Liu
Fengming Zou
Shuang Qi
Zhenquan Hu
Wenchao Wang
High Magnetic Field Laboratory, Key Laboratory of High Magnetic Field and Ion

Beam Physical Biology, Hefei Institutes of Physical Science, Chinese Academy of Sciences, Hefei, Anhui, P. R. China
Precision Medicine Research Laboratory of Anhui Province, Hefei, Anhui, P. R. China

Cheng Chen

Kailin Yu
Jiaxin Wu

Chen Hu

Juan Liu
Xuesong Liu

Li Wang

Juan Ge

High Magnetic Field Laboratory, Key Laboratory of High Magnetic Field and Ion Beam Physical Biology, Hefei Institutes of Physical Science, Chinese Academy of Sciences, Hefei, Anhui, P. R. China University of Science and Technology of China, Hefei, Anhui, P. R. China

Xiaochuan Liu

High Magnetic Field Laboratory, Key Laboratory of High Magnetic Field and Ion Beam Physical Biology, Hefei Institutes of Physical Science, Chinese Academy of Sciences, Hefei, Anhui, P. R. China

Tao Ren

Precision Medicine Research Laboratory of Anhui Province, Hefei, Anhui, P. R. China Precision Targeted Therapy Discovery Center, Institute of Technology Innovation, Hefei Institutes of Physical Science, Chinese Academy of Sciences, Hefei, Anhui, P. R. China

Mingfeng Bai

Molecular Imaging Laboratory, Department of Radiology, University of Pittsburgh Cancer Institute, University of Pittsburgh, Pittsburgh, Pennsylvania, USA

Yujiao Cai

Department of General Surgery, Second Hospital Affiliated to Army Medical University, Chongqing, P. R. China

Xudong Xiao

Department of Anesthesiology, Second Hospital Affiliated to Army Medical University, Chongqing, P. R. China

Feng Qian

Department of General Surgery, Southwest Hospital Affiliated to Army Medical University, Chongqing, P. R. China

*These authors contributed equally.

Introduction of imatinib as the first-line therapy has remarkably improved the survival of the GISTs patients, however most patients eventually experience disease progression as the development of secondary mutations in the cKIT ATP binding pocket and activation loop upon treatment.^{11,12} Sunitinib, which is approved as second-line therapy for imatinib-refractory GIST, could overcome secondary mutants in the ATP binding pocket such as V654A and gatekeeper mutant T670I, but it was insensitive to most of the mutants in the activation loop.^{13–15} Even regorafenib, which is the third-line treatment approved for imatinib-and sunitinib-resistant and intolerant GISTs, was only moderately sensitive against those secondary mutations.¹⁶ In addition, the short median progression-free survival (PFS) of sunitinib and regorafenib (6.8 months for sunitinib and 4.8 months for regorafenib) has also limited their clinical applications.^{15–17} Ponatinib and pazopanib are currently undergoing clinical investigation for GISTs and have also been demonstrated to be potent against a variety of imatinib-resistant mutants. However, safety concerns, such as high risk of arterial occlusive events for ponatinib and hypertension for pazopanib, might also restrict their clinical application.^{18,19} Hence, there is still an urgent need to develop more targeted therapies that bear different mutant sensitivity spectra and safety profiles for GISTs.

Based on high-throughput screening of the library of US Food and Drug Administration (FDA) approved drugs, we found that axitinib, a vascular endothelial growth factor receptor (VEGFR) kinase inhibitor that has been approved for the renal cell carcinoma (RCC), was sensitive to a variety of cKIT primary and secondary mutants and displayed a different mutant sensitivity spectrum compared with the clinical drugs for GISTs, including imatinib, sunitinib, and regorafenib. In this report, we describe the detailed preclinical evaluation of axitinib activity in *in vitro* and *in vivo* GISTs models bearing primary and secondary cKIT mutants.

Materials and methods

Inhibitors

Imatinib, sunitinib, regorafenib, and axitinib were purchased from a commercial chemical vendor (Haoyuan Chemexpress Inc.) and dissolved in 100% dimethyl sulfoxide (DMSO).

cKIT protein purification

The sequences encoding wild-type cKIT and T670I cKIT residues 544–935 with a Histag were cloned into baculovirus expression vector pFASTHTA. The proteins were expressed by infecting SF9 cells with high-titer viral stocks for 48 h. Cells were harvested and lysed in 25 mM Tris pH 7.4, 250 mM NaCl, and 1 mM PMSF. The supernatant was loaded to Ni-NTA Column (QIAGEN, 1018244). Then the proteins were step eluted with the same buffer with 250 mM imidazole. The eluted proteins were loaded on a Superdex-200 column equilibrated in 25 mM Tris (pH 7.4), 250 mM NaCl, 1 mM DTT, and 1 mM EDTA. Peak fractions were concentrated to 2 mg/ml and flash frozen.

Kinase biochemical assay

The ADP-Glo™ kinase assay (Promega, Madison, WI) was used to screen axitinib for its cKIT and the relevant mutation inhibition effects. The kinase reaction system contains 9 μl cKIT (12.5 ng/μl) or cKIT T670I (20 ng/μl), 1 μl of serially diluted axitinib, and 10 μl substrate Poly (4:1 Glu, Tyr) peptide (0.4 μg/μl) (Promega, Madison, WI) with 100 μM ATP (Promega, Madison, WI). The reaction in each tube was started immediately by adding ATP and kept going for an hour at 37°C. After the tube cooled for 5 min at room temperature, 5 μl solvent reactions were carried out in a 384-well plate. Then 5 μl of ADP-Glo™ reagent was added into each well to stop the reaction and consume the remaining ATP within 40 min. At the end, 10 μl of kinase detection reagent was added into the well and incubated for 30 min to produce a luminescence signal. The luminescence signal was measured with an automated plate reader (Envision, PE, USA) and the dose-response curve was fitted using Prism 5.0 (GraphPad Software Inc., San Diego, CA). The biochemical tests of other targets were provided by Invitrogen (Carlsbad, CA, USA).

Molecular modeling

All calculations were performed using the Schrödinger Suite. The DFG-out KIT complex (PDB ID: 3G0E for axitinib and 1T46 for imatinib, respectively) was used for docking studies. The crystal structure were prepared using the Protein Preparation Wizard and the T670I/V654A mutant were modeled *in situ* within Maestro. The ligand structures were built in Maestro and prepared for docking using LigPrep

(LigPrep 3.4, Schrödinger, LLC, New York, NY) and further docked into the receptor by the IFD protocol (Induced Fit Docking protocol, Schrödinger, LLC, New York, NY).

Cell lines and cell culture

The human GIST-T1 cell line was purchased from Cosmo Bio Co., Ltd, Tokyo, Japan. GIST-882 and GIST-48B cell lines were kindly provided by the group of Professor Jonathan A. Fletcher, Brigham and Women's Hospital in Boston, USA. GIST-5R cell line, carrying an additional missense mutation encoding KIT T670I (exon 14), was derived from imatinib-resistant colony of GIST-T1 cell line, which was kindly provided by the group of Professor Brian Rubin in Lerner Research Institute, USA.²⁰ Isogenic Ba/F3 cells lines were cultured in RPMI 1640 media (Corning) with 10% fetal bovine serum (FBS, Gibco) and supplemented with 2% L-glutamine and 1% penicillin/streptomycin. GIST-T1 and GIST-5R cells were maintained in DMEM (Corning) supplemented with 10% FBS and 1% penicillin/streptomycin. GIST-882 and GIST-48B were grown in IMDM (Corning) supplemented with 10% FBS and 1% penicillin/streptomycin. All cell lines were maintained in culture media at 37°C with 5% CO₂.

Ba/F3 isogenic cell line generation

Retroviral constructs for Ba/F3-KIT mutants were made based on the pMSCVpuro (Clontech) backbone. For TEL-KIT vector, the first 1 kb of human TEL gene with an artificial myristylation sequence (MGCGCSSHPEDD) was cloned into the pMSCVpuro retroviral vector, followed by a 3×FLAG tag sequence. Then, the kinase domain coding sequence of KIT was inserted in-frame between TEL and 3×FLAG sequences. For full-length expression vectors, the coding sequences of KIT variants were directly cloned in pMSCVpuro vector with a 3×FLAG tag at the C-terminal end. All mutagenesis was performed using the QuikChange Site-Directed Mutagenesis Kit (Stratagene) following the manufacturer's instructions. Retrovirus was packaged in HEK293T cells by transfecting KIT-containing MSCV vectors together with two helper plasmids. Virus supernatants were harvested 48 h after transfection and filtered before infection. Then Ba/F3 cells were infected with harvested virus supernatants using spinoculation protocol, and stable cell lines were

obtained by puromycin selection for 48 h. The IL-3 concentrations in the culture medium were gradually withdrawn until cells were able to grow in the absence of IL-3.

Cell proliferation assays

Cells were seeded in 96-well culture plates for proliferation assay. For isogenic cells, GIST-T1, GIST-48B, and GIST-5R cells, the seeding number is 2500–3000 cells per well. For GIST-882 cells, the seeding number is 5000 cells/well. For adherent cell lines, compounds of various concentrations were added into the plates after cells were cultured for 12 h. For cell lines, cell proliferation was determined after treatment with compounds for 72 h. For primary cells, cell proliferation was determined after treatment with compounds for 6 days. Cell viability was measured using the Cell Titer-Glo assay (Promega, USA) according to the manufacturer's instructions, and luminescence was measured in a multilabel reader (Envision, PerkinElmer, USA). Data were normalized to control groups (DMSO) and represented by the mean of three independent measurements with standard error <10%. GI₅₀ values were calculated using Prism 5.0 (GraphPad Software, San Diego, CA).

Colony formation assay

GIST-T1, GIST-882, GIST-48B, and GIST-5R cells were trypsinized and dispensed into individual wells of six-well tissue culture dishes with a density of 50,000 cells per well. Cells were maintained in a humidified 5% CO₂ incubator at 37°C for 15 days, and continuously treated with serially diluted axitinib, imatinib, sunitinib, and regorafenib. On the 15th day, the numbers of colonies in each well were quantified and each measurement was performed in triplicate. The data were normalized to vehicle treatment and quantification was analyzed by Image J software (National Institutes of Health, USA).

Signaling pathway examination

GIST-T1, GIST-882, GIST-5R, and GIST-48B cells were treated with DMSO, serially diluted axitinib, 1 μM imatinib, and 1 μM sunitinib for 1 h. Cells were then washed with cold PBS and lysed in RIPA buffer (Beyotime, China) with a protease inhibitor cocktail (Roche). Immunoblotting was performed by standard protocols. The following antibodies were used at a range of antibody

concentrations as indicated by the manufacturers to probe for specific proteins: phosphorylated KIT (Tyr719), KIT (Tyr703), AKT (Ser473), AKT (Thr308), STAT3 (Ser705), STAT5 (Tyr694), ERK1/2 (Thr202/Tyr204), and p70 S6K(Thr 389) were all from Cell Signaling Technology. Rabbit polyclonal antibody to phosphorylated KIT (Tyr823) was from Invitrogen. β -actin antibody was purchased from Sigma.

Cell cycle analysis

GIST-T1, GIST-882, GIST-5R, and GIST-48B cells were treated with DMSO, serially diluted axitinib (0.3, 1, and 3 μ M), 1 μ M imatinib, and 1 μ M sunitinib for the indicated periods. The cells were fixed in 70% cold ethanol and incubated at -20°C overnight then stained with PI/RNase staining buffer (BD Pharmingen). Flow cytometry was performed using a FACS Calibur (BD), and results were analyzed by ModFit software.

Apoptosis effect examination

GIST-T1, GIST-882, GIST-5R, and GIST-48B cells were treated with DMSO, serially diluted axitinib, 1 μ M imatinib, and 0.1 μ M sunitinib for the indicated periods. Cells were collected and analyzed by Western blotting using the following antibodies: PARP and caspase-3 from Cell Signaling Technology. β -actin antibody was purchased from Sigma.

GIST-T1, GIST-5R xenograft, and Ba/F3 cKIT-V654A allograft tumor models

Four-week old female BALB/c-nu/nu mice were purchased from Nanjing Biomedical Research Institute of Nanjing University (Nanjing City, Jiangsu Province, China). All animals were maintained in the Animal Center of Hefei Institutes of Physical Science, Chinese Academy of Sciences according to the Guide for the Care and Use of Laboratory Animals (National Research Council [US] Committee).²¹ All the experimental protocols were approved by the Hefei Institutes of Physical Science ethics committee, Chinese Academy of Sciences (approval number HFCASDWLL20160510). Prior to implantation, cells were harvested during exponential growth. Five million cells (GIST-T1 and GIST-5R) and one million cells (Ba/F3 cKIT-V654A) in PBS were formulated as a 1:1 mixture with Matrigel (BD Biosciences) and injected into the subcutaneous space on the right flank of nu/nu mice. Daily

oral administration was initiated when tumors had reached a size of 200–400 mm³. Animals were then randomized into treatment groups of five or six mice each for efficacy studies. Axitinib was delivered daily in a HKI solution (0.5% Methocellulose/0.4% Tween80 in ddH₂O) by orally gavage. A range of doses of axitinib or its vehicle were administered, as indicated in figure legends. Body weight and tumor growth were measured daily after axitinib treatment. Tumor volumes were calculated as follows: tumor volume (mm³) = [(W² × L)/2] in which width (W) is defined as the smaller of the two measurements and length (L) is defined as the larger of the two measurements. The TGI were calculated according to actual tumor weight using the formula: $(W_{\text{Vehicle}} - W_{\text{Test}})/W_{\text{Vehicle}} \times 100\%$ in which W is defined as actual tumor weight.

GISTs tumor sample processing

This study was reviewed and approved by the Research Ethics Committees of The People's Liberation Army joint logistics support force No. 901 Hospital (approval number 2018A026). The written informed consent was obtained from all patients who take part in the study. The protocol was carried out in accordance with Good Clinical Practice standards and the Declaration of Helsinki. Briefly, patient resections were placed in a sterile conical tube containing DMEM media (Invitrogen) with 5% antibiotic–antimycotic (Fisher Scientific) on wet ice during transport from the operating room to the research laboratory. Fragments of freshly obtained tumor tissues were dissociated using collagenase/hyaluronidase and dispase (StemCell Technologies) at 37°C for 2 h with shaking in 37°C as described previously.²² Primary cells were then placed in flasks coated with collagen I (Corning) in culture medium. The culture medium included DMEM/F12 medium with freshly added supplements: 5% FBS (Gibco), primocin (Invivogen), Glutamax-I (Gibco), 25 μ g/ml hydrocortisone (Sigma), 125 ng/ml EGF (Sigma), 5 μ g/ml insulin (Gibco), and 10 μ M Rho kinase inhibitor Y27632 (Haoyuan Chemexpress Inc.) in humidified 37°C/5% CO₂ incubators at 2% O₂. Medium was replaced every 3 days and the primary cells were cultured for a period of 3–4 weeks. All the experiments were conducted using low-passage primary cultures.

Whole transcriptome shotgun sequencing

RNA was purified with RNeasy Plus Micro Kit (Qiagen), Qubit and the Agilent BioAnalyzer

technologies were used to qualify and control the quality of RNA: 500 ng RNA [RNA integrity number (RIN) >7] from each sample was used for library construction with NEBNext Ultra RNA library prep kit (NEB) according to the manufacturer's instructions. The samples were barcoded and run on a Novaseq platform in a 100 base-pair (bp) paired-end run. An average of 20 million paired reads was generated per sample.

Immunofluorescence

GIST cell lines and primary GIST cells were grown on coverslips and treated with compounds of various concentrations for the indicated time. Cells were washed once with PBS and fixed by 4% formaldehyde at room temperature for 20 min. Then they were blocked by AbDil-Tx (TBS-Tx supplemented with 2% BSA and 0.05% sodium azide) at room temperature for 1 h, followed by c-KIT (Cell Signaling Technology), CD34 (Abcam), DOG1 (Cell Signaling Technology), β -Tubulin (Cell Signaling Technology), or Aurora A (Cell Signaling Technology) antibody incubation at 4°C overnight. Secondary antibodies were conjugated to either Alexa Fluor 488 or Alexa Fluor 594 (Life Technologies) and mounted by antifade prolong Gold with DAPI (Life Technologies). Fluorescence was measured by a Leica (DMI4000B) fluorescent microscope. Images are representative of at least three independent images.

Immunohistochemistry stain

Tumor tissues were fixed in 10% neutral-buffered formalin and embedded in paraffin. Six-micrometer tissue sections were prepared, deparaffinized, dehydrated, and then stained with hematoxylin and eosin (H&E) using routine methods. Commercially available primary antibody to human Ki-67 (ZSGB-BIO, Beijing, China) was used for Ki-67 staining. After heat-induced antigen retrieval, formalin-fixed and paraffin-embedded tumor tissue sections were stained with primary antibody overnight at 4°C. The slides were subsequently incubated with ImmPRES anti-mouse Ig (Vector Laboratories, Burlingame, CA) at room temperature for 30 min, stained with peroxidase substrate 3,3'-diaminobenzidine chromogen (Vector Laboratories, Burlingame, CA), and finally counterstained with hematoxylin. TUNEL staining was assessed using an *in situ* Cell Death Detection Kit (POD)

(Roche, Mannheim, Germany) according to the manufacturer's instructions.

Statistical analyses

All statistical analyses were performed using Graph Pad Prism software (GraphPad Software Inc., La Jolla, CA, USA). Three independent replicates were performed for each experiment. Data are presented as mean \pm standard deviation (SD), with *n* indicating the number of replicates. Differences between groups were assessed by a paired *t* test and accepted as significant at *p* < 0.05.

Results

In vitro inhibitory activity of axitinib against a panel of cKIT kinase primary and secondary mutants

We first examined axitinib on a panel of cKIT kinase primary and secondary mutants transformed Ba/F3 cells by comparing with imatinib, sunitinib, and regorafenib [Figure 1(a) and Supplemental Table 1]. The results demonstrated that axitinib was active to cKIT wild type (GI₅₀: 50 nM). For the JM domain primary mutants such as L576P and V559D/A/G, axitinib displayed better potencies than imatinib, sunitinib, and regorafenib. Like sunitinib and regorafenib, axitinib could also inhibit the imatinib-resistant gatekeeper mutant T670I (GI₅₀: 108 nM) and JM domain/ATP binding pocket combined mutants T670I/V559D (GI₅₀: 191 nM), although it was less potent than sunitinib. Interestingly, axitinib showed similar potencies to sunitinib against another imatinib resistant mutant V654A in ATP binding pocket (GI₅₀: 5 nM) and combined mutants V654A/V559D (GI₅₀: 20 nM), and the efficacy is better than regorafenib. In addition, axitinib performed better than imatinib, sunitinib, and regorafenib on the secondary mutants A829P in the activation loop. These results suggested that cKIT wild type, JM domain primary mutants L576P and V559D/A/G, imatinib-resistant mutants V654A in the ATP binding pocket are sensitive to axitinib and the mutant in the activation loop A829P was also sensitive to axitinib, compared with imatinib, sunitinib, and regorafenib.

Given the fact that all of these inhibitors are multiple-target compounds and in order to confirm the on-target effects on those transformed Ba/F3

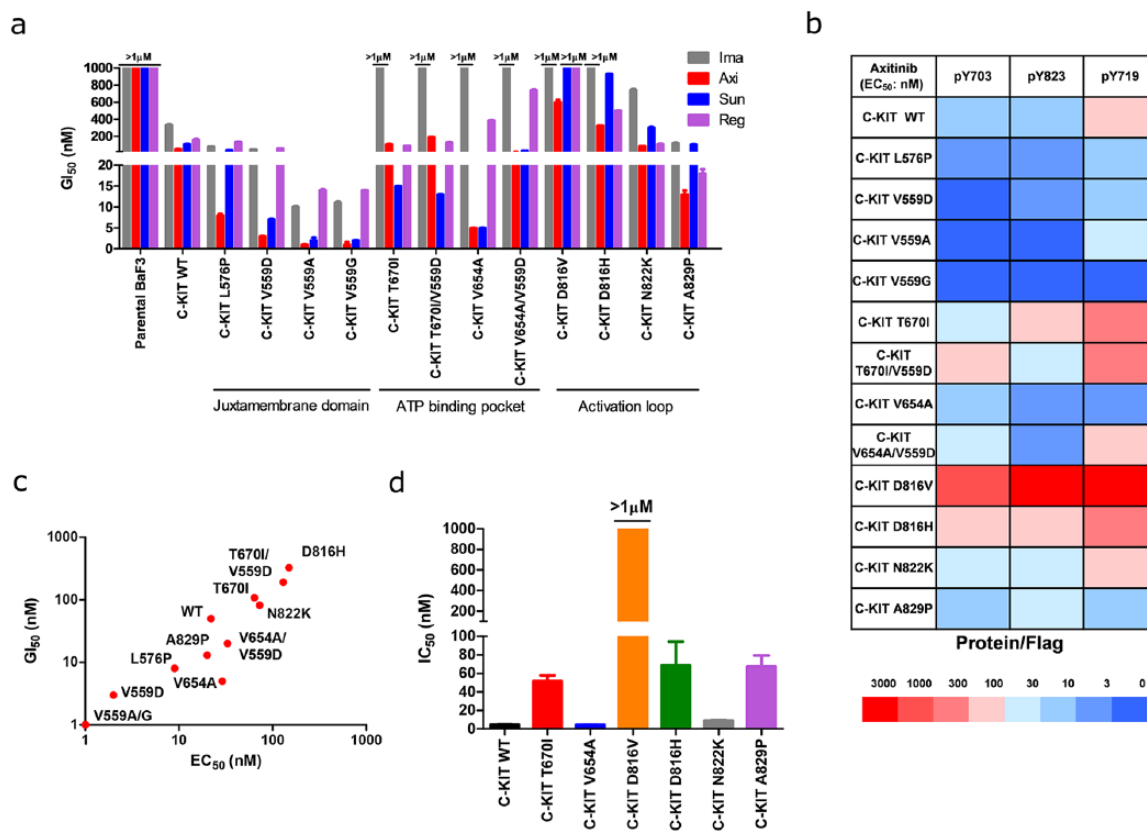


Figure 1. Axitinib inhibits a panel of cKIT mutants *in vitro*. (a) GI₅₀ values (nM) of axitinib, imatinib, sunitinib, and regorafenib in Ba/F3 isogenic cell lines harboring mutants in juxtamembrane domain, ATP binding pocket, and activation loop of cKIT kinase. The cell lines were treated with increasing concentrations of drugs for three days followed by cell viability assessment using the Cell Titer-Glo assay. The mean \pm SD is shown. (b) Heatmap showing EC₅₀ values calculated by quantifying the protein levels of different phosphorylation sites of cKIT in Ba/F3 isogenic cell lines after axitinib treatment. Red indicates high whereas blue indicates low EC₅₀ values. (c) The correlation between GI₅₀ and EC₅₀ values in Ba/F3 isogenic cell lines. (d) Biochemical assay of axitinib against different cKIT mutant proteins. IC₅₀ values (nM) of axitinib were obtained in three separate studies.

cells, we then assessed KIT Y703, Y719, and Y823 phosphorylation in axitinib-treated Ba/F3 cells [Figure 1(b) and Supplemental Figure 1]. The results showed that axitinib could potentially inhibit the most common cKIT phosphorylation site Y703² of the cKIT wild type, primary mutants L576P and V559D/A/G within the JM domain, secondary mutants V654A and V654A/V559D within the ATP binding pocket, as well as secondary mutant A829P within the activation loop. It was less potent *versus* the drug-resistant secondary mutant T670I and T670I/V559D within the ATP binding pocket. Not surprisingly, it had lower potency against the activation loop mutants such as D816H and lowest potency against the D816V mutant. The EC₅₀s correlate with the GI₅₀s of axitinib in these cells [Figure 1(c)]. In addition, we also examined the inhibitory activity of axitinib against purified cKIT wild type and

mutant proteins in the biochemical enzymatic assay with Invitrogen's SelectScreen technology [Figure 1(d)]. The results showed that axitinib was potent against cKIT wild type (IC₅₀: 4.78 nM), cKIT V654A mutant (IC₅₀: 4.56 nM), and cKIT N822K (IC₅₀: 9.12 nM) but relatively less potent against cKIT T670I (IC₅₀: 51.8 nM), A829P (IC₅₀: 67.3 nM), and D816H (IC₅₀: 68.6 nM) mutants and much less potent against D816V mutant (IC₅₀: 1050 nM), which is in accordance with the antiproliferative effect observed in the transformed Ba/F3 cells and further confirmed the on-target effect of axitinib.

Structural basis of the sensitivity of axitinib against cKIT-V654A and T670I mutants

In order to better understand the structural basis of the sensitivity of axitinib, we then docked it

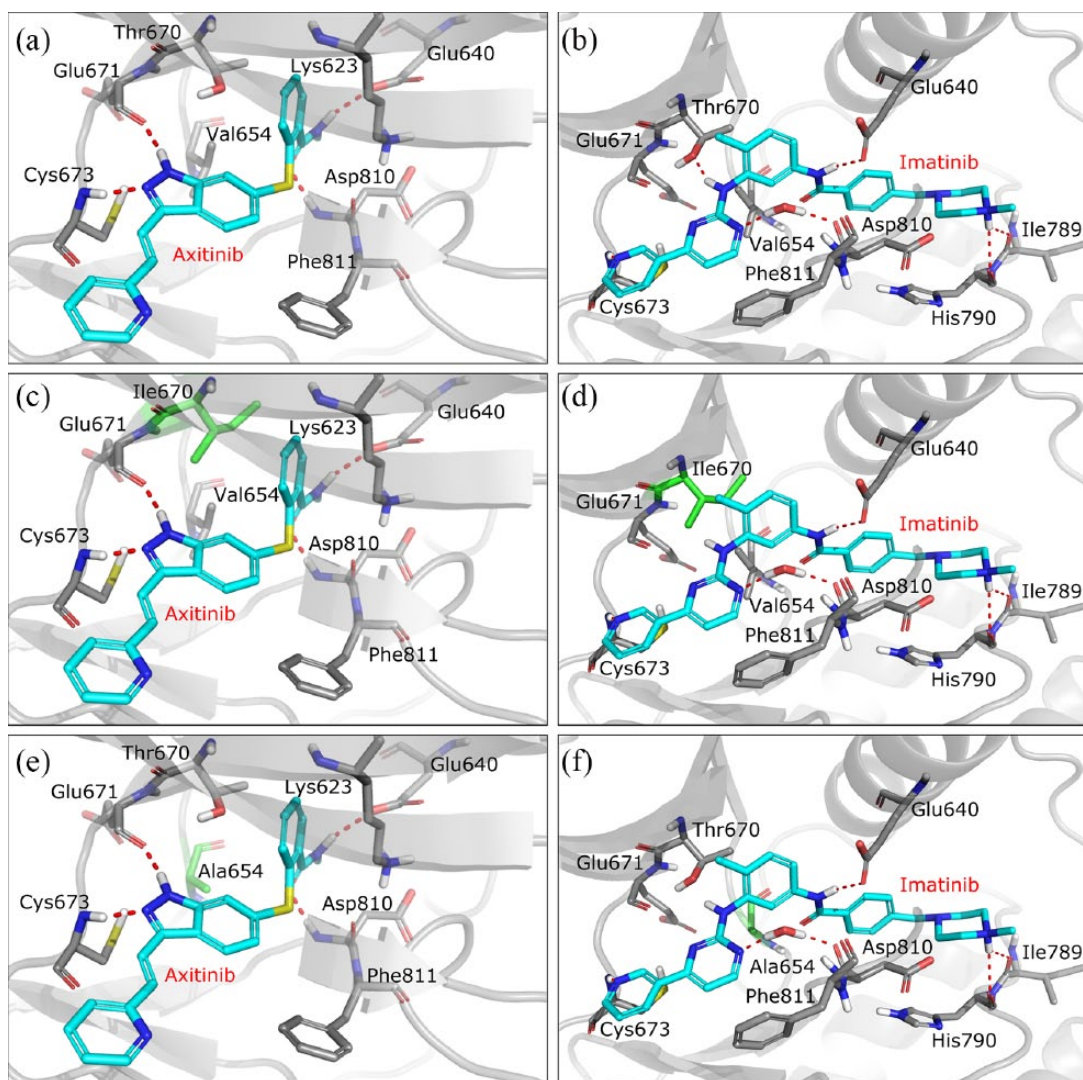


Figure 2. Structural binding mechanism of axitinib and imatinib. (a) Analysis of the cKIT wild type/axitinib binding mode (PDB ID: 3G0E). (b) X-ray crystal structure of cKIT wild type/imatinib (PDB ID: 1T46). (c) Analysis of the cKIT T670I/axitinib binding mode (PDB ID: 3G0E). (d) Analysis of the cKIT T670I/imatinib binding mode (PDB ID: 1T46). (e) Analysis of the cKIT V654A/axitinib binding mode (PDB ID: 3G0E). (f) Analysis of the cKIT V654A/imatinib binding mode (PDB ID: 1T46).

into cKIT wild type, T670I, and V654A mutants in comparison with imatinib. The results showed that axitinib adopted a typical type II binding mode to cKIT wild-type protein, featuring a DFG-out inactive conformation, which is similar to imatinib [Figure 2(a) and (b)]. The indazole ring formed two hydrogen bonds with Cys673 and Glu671 in the hinge binding region. The methyl benzamide formed two canonical hydrogen bonds with Glu640 located in the c-Helix region and Asp810 located in the DFG motif. When threonine 670 mutated into isoleucine (T670I), it did not affect the binding of axitinib

because the cave created by the thio-bridged two phenyl rings was big enough to accommodate the larger isoleucine residue [Figure 2(c)]. However, the T670I mutant not only lost one of the hydrogen bonds formed by Threonine, but also introduced a steric hindrance by isoleucine, which made it remarkably disfavored for the binding to imatinib [Figure 2(d)]. The V654A mutant did not affect the binding of axitinib because the residue at this position has no direct hydrophobic interaction with the drug [Figure 2(e)]. However, for imatinib, the smaller residue Ala weakened the favorable hydrophobic interaction generated

by the relatively larger residue Val. Therefore, the mutation resulted in activity loss, although it was not as significant as T670I mutant [Figure 2(f)].²³

In vitro activity of axitinib in GISTs cell lines harboring primary and secondary mutants

We next examined the antiproliferative effect of axitinib against a panel of established GIST cancer cell lines [Figure 3(a)]. As expected, among four drugs we tested, axitinib was the most potent to GIST-T1 (GI₅₀: 21 nM), which harbors a primary mutation in the JM domain (Δ 560–578). It also displayed similar potency to imatinib and sunitinib against GIST-882, which harbors K642E mutant in the c-Helix of the ATP binding pocket but was more potent than regorafenib. In addition, axitinib was more sensitive than regorafenib to the imatinib resistant GIST-5R cells, which carry an additional missense mutation encoding KIT T670I (exon 14), but less sensitive than sunitinib. For GIST-48B, a cKIT-independent cell line, none of them exhibited good activity. These growth inhibition efficacies also correlated well with the results in colony formation assays [Figure 3(b)].

In order to further confirm the on-target effect of axitinib on these cell lines, we next determined the signaling pathway response upon treatment [Figure 4(a)]. In the GIST-T1 and GIST-882 cells, it could potently inhibit phospho-cKIT Y719, Y703, and Y823 and the downstream signaling mediators including phospho-AKT, phospho-S6K, phospho-S6, phospho-ERK, phospho-STAT3, and phospho-STAT5. Interestingly, in the cKIT T670I cell line GIST-5R, neither axitinib nor sunitinib displayed great inhibitory effect against phospho-cKIT Y719, but both of them still potently inhibited phospho-cKIT Y703, Y823, and downstream phospho-AKT, ERK, S6K, S6, STAT3, and STAT5. In the KIT-independent cell line GIST48B, no detectable levels of phosphorylated KIT and minimal levels of total KIT were found. The downstream mediators of cKIT signalling pathway were not affected obviously after axitinib treatment.

Axitinib induced the cell cycle arrest and apoptosis in GISTs cell lines

We then examined the effects of axitinib on cell cycle progression and apoptosis. Not surprisingly, axitinib blocked cell cycle progression at G0/G1 phase at 0.3 μ M in the drug-sensitive cell lines including GIST-T1, GIST-882, and GIST-5R,

but not in the insensitive cell line GIST-48B. While starting from 1 μ M, the cell cycle was arrested at G2/M phase in all of the cell lines we tested [Figure 4(b)]. This may due to the aurora kinase activity of axitinib (K_d of aurora A:B:C = 72, 11, and 1.3 nM respectively).^{24,25} To confirm that, we performed immunofluorescence examination (Supplemental Figure 2). The results were supportive of the cell cycle data, with the centrosome separation and spindle assembly being interrupted by axitinib treatment. Axitinib also induced apoptosis in KIT mutant GIST cell lines in a dose-dependent manner, but not in GIST-48B by examining cleaved PARP and caspase-3 [Figure 4(c)]. These results were in accordance with the growth inhibition effects observed in those GIST cell lines.

Axitinib suppressed the tumor growth of GIST-T1, GIST-5R, and cKIT-V654A Ba/F3 cells mediated mouse model

To further investigate the potential of the clinical application of axitinib, we then examined its *in vivo* efficacies in several different preclinical models. In the GIST-T1 and GIST-5R cells inoculated xenograft mouse models and the cKIT-V654A Ba/F3 inoculated allograft mouse model, oral administration of axitinib at different dosages (25, 50, and 100 mg/kg/day) did not show any apparent toxicity (Supplemental Figure 3). In the GIST-T1 xenograft mouse model, axitinib exhibited dose-dependent tumor growth suppression and the TGI (tumor inhibition rate) was 53% at 100 mg/kg/day dosage [Figure 5(a)]. In the GIST-5R xenograft mouse model, 100 mg/kg/day dosage of axitinib could almost completely block the tumor progression and showed a TGI of 88%, whereas the same dosage of imatinib showed limited effect on tumor growth [Figure 5(b)]. As expected, reduced phosphorylation of cKIT and related downstream mediators such as STAT3, AKT, and ERK in tumors were observed compared with the vehicle-treated controls (Supplemental Figure 4). Furthermore, we found that at 100 mg/kg dosage, aurora kinase started to be inhibited, which might help to enhance the antitumor efficacy of axitinib *in vivo* (Supplemental Figure 4). These data were also consistent with the results we observed in the cell cycle arrest assays and centrosome separation experiments [Figure 4(b) and Supplemental Figure 2]. In the cKIT-V654A Ba/F3 inoculated allograft mouse model, axitinib also showed a dose-dependent tumor growth inhibition. Even at 25 mg/kg/day dosage, the TGI achieved was 66.8%, whereas

a

Cell line (GI ₅₀ :nM)	KIT status	Imatinib	Axitinib	Sunitinib	Regorafenib
GIST-T1	Δ560-578	47±4	21±2	27±1	149±3
GIST-882	K642E	170±5	152±2	200±4	350±7
GIST-48B	KIT-independent	>10000	2020±33	3124±72	7090±81
GIST-5R	Δ560-578/T670I	>10000	400±5	47±3	847±12

b

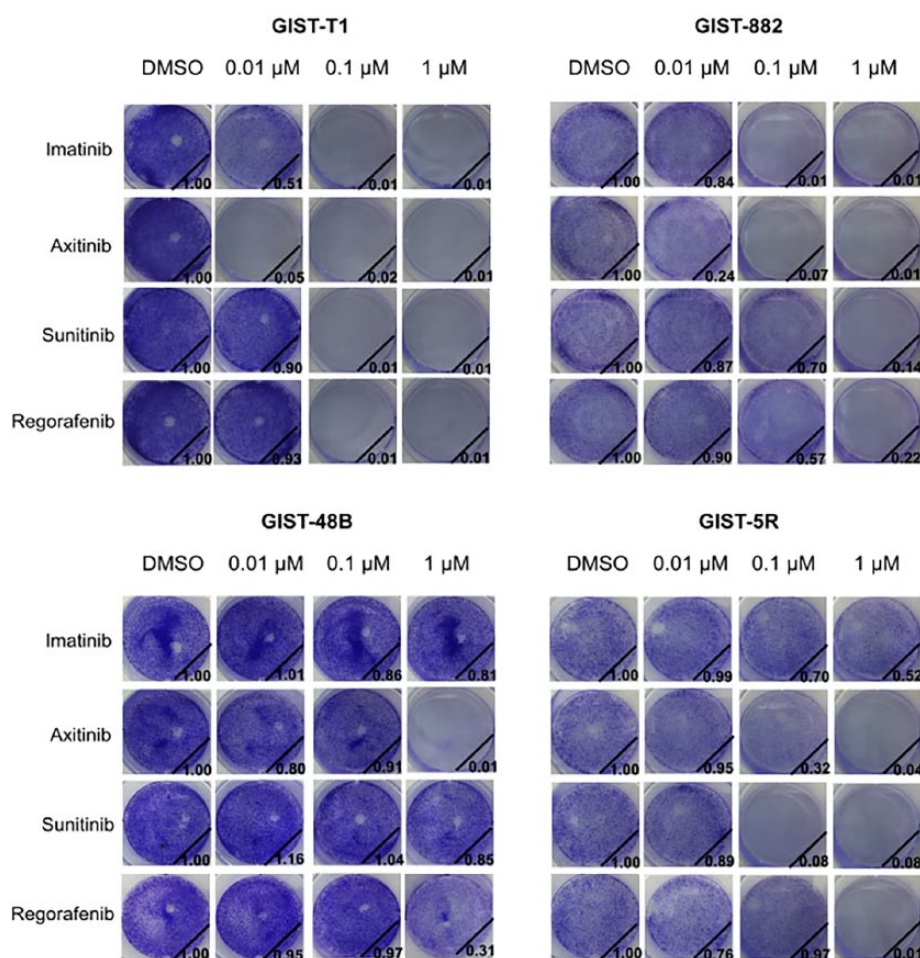


Figure 3. Axitinib inhibits the proliferation of human GIST cancer cell lines. (a) GI₅₀ values (nM) of axitinib, imatinib, sunitinib, and regorafenib in four human GIST cell lines relative to DMSO-treated control after 72 h treatment. Cell viability was assessed using the Cell Titer-Glo assay. (b) Crystal violet staining of colonies from the four human GIST cell lines treated for 15 days with the indicated doses of axitinib, imatinib, sunitinib, and regorafenib. Normalized cell colonies number quantification (relative to vehicle control) is shown at bottom right of each plate.

imatinib did not show significant inhibition on tumor growth [Figure 5(c)]. Immunohistochemical (IHC) staining results showed that axitinib

dose-dependently inhibited proliferation (Ki-67 stain) and induced apoptosis (TUNEL stain) in all three mouse models (Supplemental Figure 5).

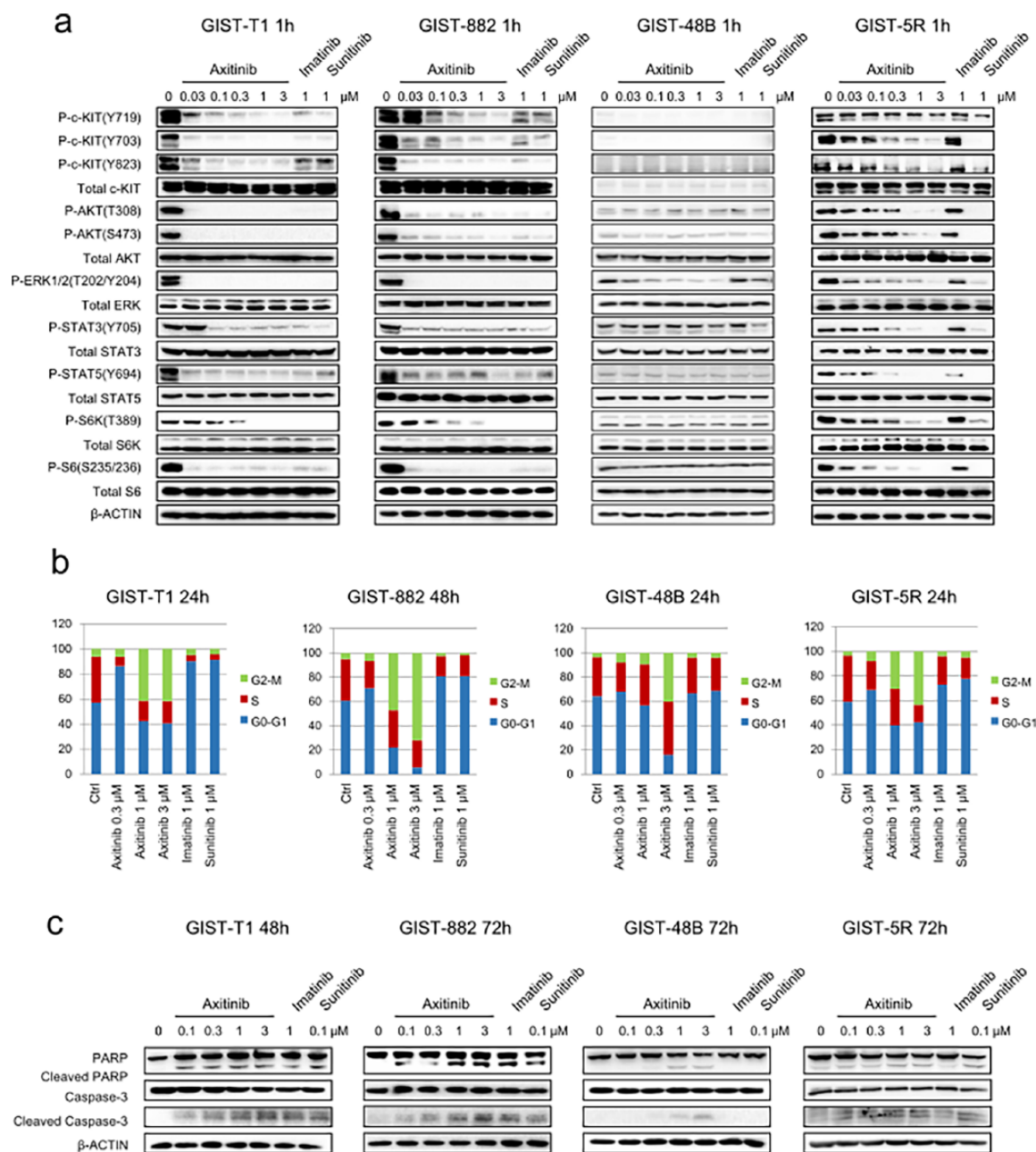


Figure 4. The effects of axitinib on cellular signaling, cell cycle progression, and apoptosis in human gastrointestinal stromal tumor (GIST) cancer cell lines. (a) Immunoblotting analysis of indicated proteins in c-KIT mediated signaling pathways of GIST-T1, GIST-882, GIST-48B, and GIST-5R cell lines. (b) Cell cycle analysis of the effect of axitinib with different concentrations in human GIST cell lines measured by flow cytometry. Imatinib and sunitinib were used as positive controls. (c) Immunoblotting analysis of apoptosis-related proteins after axitinib treatment in human GIST cell lines. Imatinib and sunitinib were used as positive controls.

Axitinib is effective in human GIST patient-derived primary cells

We next tested the effects of axitinib in a more physiological setting in an *ex vivo* culture of human GIST patient-derived primary cells (Supplemental Table 2). We observed that *ex*

in vivo culturing of patient A's primary cells for 6 days in the presence of axitinib (1 μM) substantially decreased both the cKIT-positive and CD34-positive GIST patient-derived primary cells [Figure 6(a)]. These results were confirmed using another GIST IHC marker DOG1 [Figure

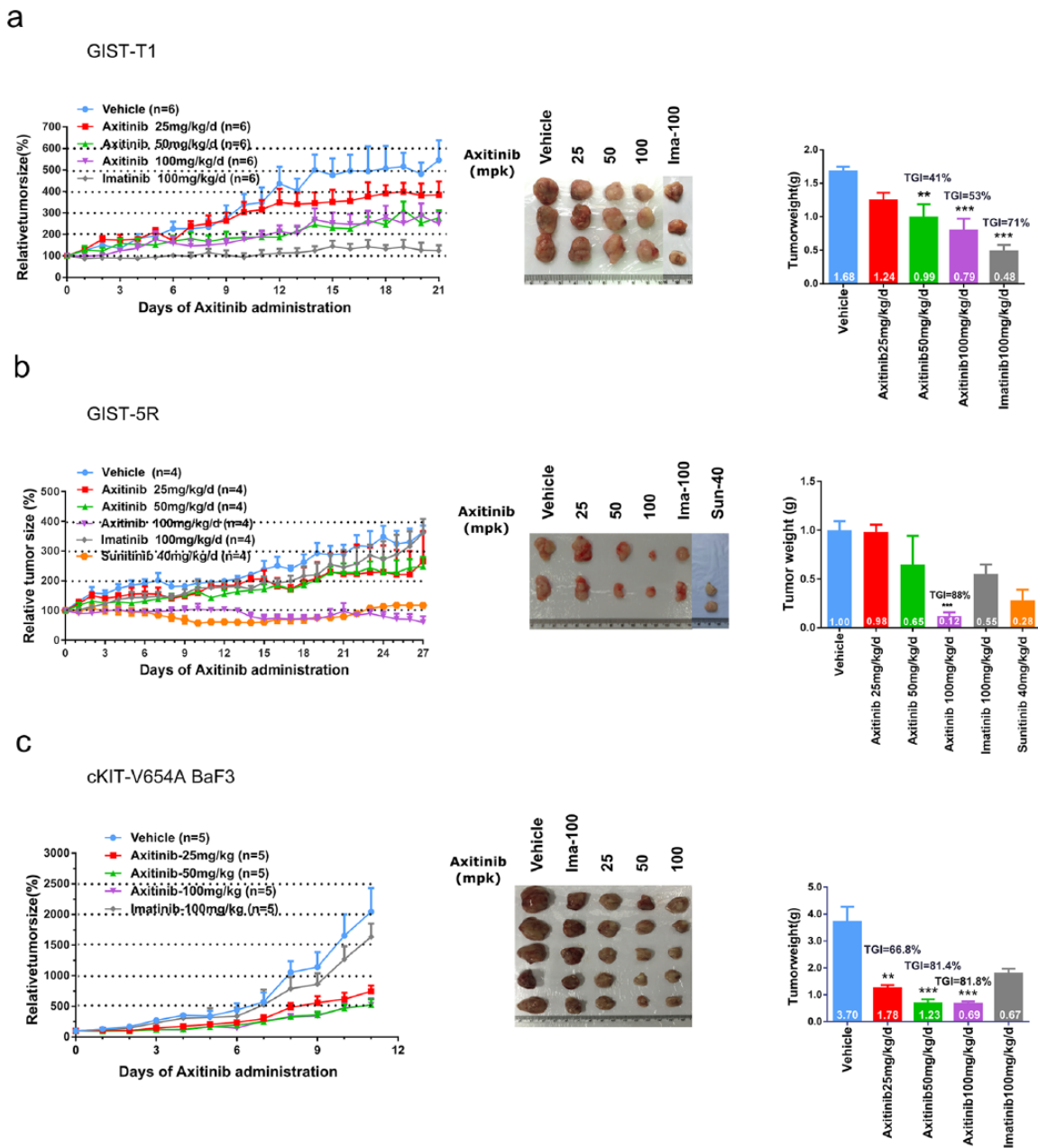


Figure 5. Axitinib inhibits tumor growth of GIST-T1, GIST-5R-inoculated xenograft mouse models, and Ba/F3 cKIT-V654A cell-inoculated allograft mouse model *in vivo*. The effect of axitinib on tumor size and tumor weight in (a) GIST-T1 inoculated mouse xenograft model, (b) GIST-5R inoculated mouse xenograft model, and (c) Ba/F3 cKIT-V654A cell-inoculated mouse allograft model. Tumor-bearing animals were treated once daily by oral gavage with vehicle or the indicated dose of drug for the indicated dosing period. Mean tumor volume and standard deviation are plotted. Statistical significance, calculated using Student's *t* test in which each treatment group was compared with its vehicle control, is indicated by asterisk. * $p < 0.05$, ** $p < 0.01$, *** $p < 0.001$.

6(b)] indicating that axitinib indeed exhibited an antiproliferative effect on the patient-derived primary cells of GIST.

In order to further quantify these effects, we next tested the antiproliferation effect of axitinib on the

other three GIST patients. Patients B and C harbored cKIT-V599D and cKIT-K642E mutation, respectively, and were evaluated by whole-transcriptome sequencing, whereas there is no cKIT mutation in patient D's primary cells (Supplemental Table 3). The results demonstrated that the viability

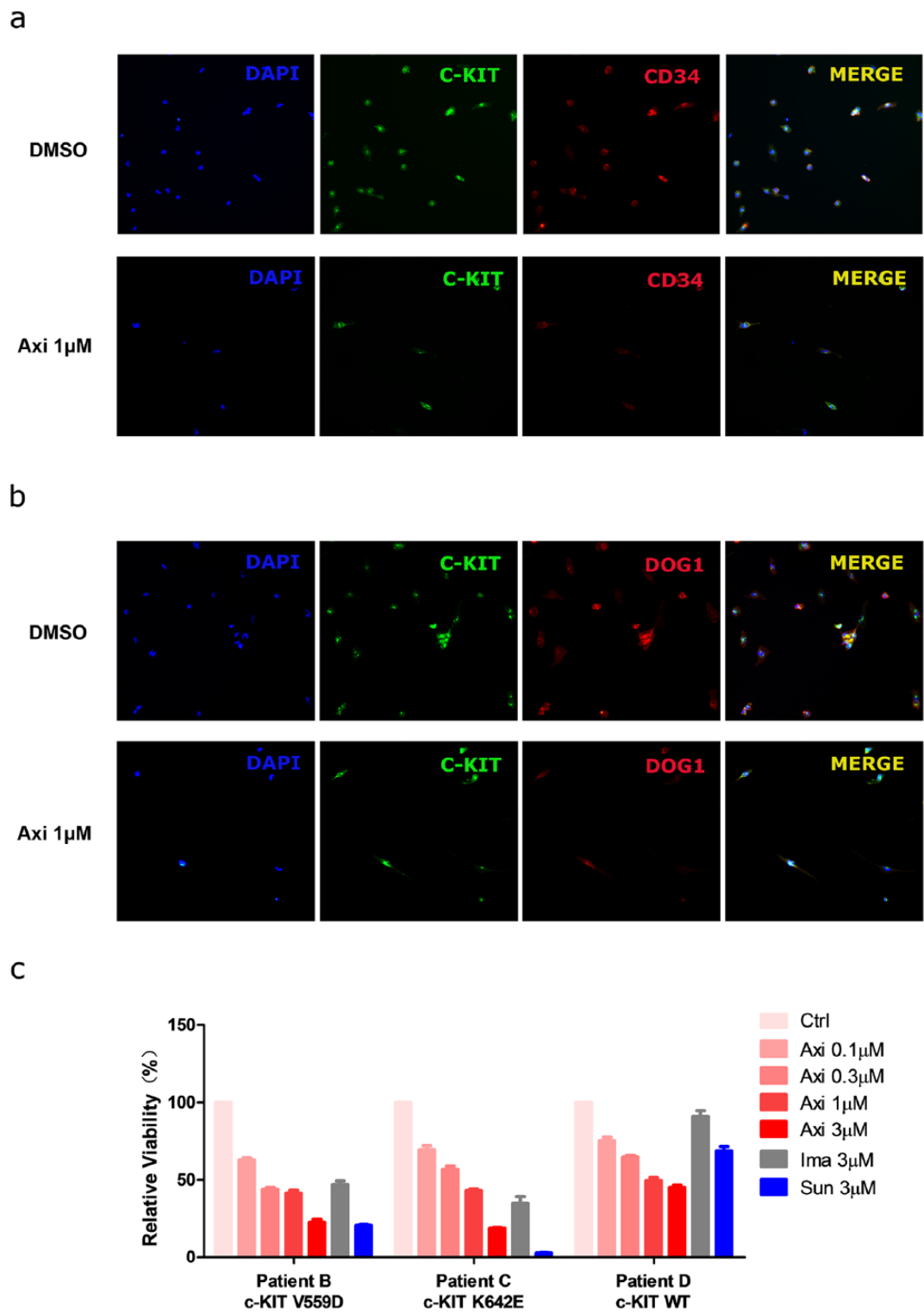


Figure 6. The effect of axitinib on gastrointestinal stromal tumor (GIST) patient-derived primary cells. (a) Immunofluorescence stain for cKIT (green), CD34 (red), and DAPI (blue) in representative sensitive GIST patient-derived primary cells *ex vivo* treated with axitinib (1 µM) for 6 days. (b) Immunofluorescence stain for cKIT (green), DOG1 (red), and DAPI (blue) in representative sensitive GIST patient-derived primary cells treated with axitinib (1 µM) for 6 days. (c) Cell viability assessment of primary cells from three GIST patients, relative to DMSO-treated condition, after 6 days of treatment with axitinib of different concentrations using Cell Titer-Glo assay. Imatinib and sunitinib were used as positive control. The mean ± standard deviation is shown.

of these primary cells was inhibited by axitinib dose-dependently in all three patient samples [Figure 6(c)], consistent with our previous data in GIST cell line models. Interestingly, patient D, harboring cKIT wild type, responded to axitinib whereas imatinib and sunitinib did not display potent inhibition even at 3 μM concentration. We speculated that aurora kinase inhibition might contribute to this efficacy because starting from 1 μM concentration axitinib could induce G2/M arrest and centrosome separation interruption, which was different from other cKIT kinase inhibitors [Figure 4(b) and Supplemental Figure 2]. To confirm this result, we also examined the signaling pathway in the primary cells from patient D. The results showed that both the phospho-cKIT and phospho-Histone H3, which is the downstream substrate of aurora kinase and a widely used marker for aurora kinase inhibition efficacy,^{26–28} were potently inhibited by axitinib at 1 μM (Supplemental Figure 6). These results revealed that at higher concentration, the aurora kinase inhibition would also contribute to the antiproliferation effect of axitinib.

Discussion

With the development of the next-generation sequencing, more and more primary gain-of-function mutations and drug-resistant mutations are being identified from patients in the clinic. For instance, more than a dozen different cKIT mutations have already been found in GIST patients.²⁹ Although there have been three different targeted drugs approved for GISTs, in the precision medicine era that each specific mutant may require a specific corresponding treatment to achieve optimal clinic response for the individual patient, there remains a clear need for more agents that display different target-sensitive spectra to overcome or suppress the different resistance mutations of cKIT that have emerged in GIST patients.

In this study, through applying drug repurposing strategies, we have identified axitinib, which has been approved for the clinical use in RCC, is sensitive against a panel of primary gain-of-function cKIT mutants and secondary drug-resistant mutants. Meanwhile, it exhibited a different drug sensitivity spectrum compared with sunitinib and regorafenib. We assessed the effects of axitinib in 13 engineered Ba/F3 cell lines, 4 GIST cell lines, and 4 GIST patient-derived primary cell models, with consistent results observed across these different model systems. We also analyzed the binding mode of the KIT kinase and axitinib, with

comparisons with the KIT/imatinib structure to provide a structural basis of the KIT inhibitory profile of axitinib. As axitinib has been clinically used and the concentration in human (5–10 mg b.i.d. dosage would provide a C_{max} around 250 nM concentration³⁰) could cover the IC_{50} range of axitinib against most cKIT primary mutants and imatinib-resistant mutants including T670I and V654A, we envisioned that it might have the potential for application in the clinic.

In the GIST patient-derived primary cells with wild-type c-KIT (lacking cKIT mutation), imatinib and sunitinib were not sensitive to these primary patient cells, which was also reported in the clinic.^{31–33} Interestingly, we found axitinib displayed drug response in these wild-type c-KIT GIST primary cells. After examined the signaling pathway in patient D, we found that both phospho-cKIT and the downstream marker of aurora kinase, phospho-HH3(S10), were inhibited after axitinib treatment. Therefore, we speculate that at relatively lower concentrations (concentration less than 1 μM , which could cover the IC_{50} ranges of the axitinib against most cKIT mutants), axitinib mainly exerts its efficacy through the cKIT inhibition, whereas at higher concentrations, aurora kinase inhibition might help to enhance the antiproliferative effect of axitinib. Hence, our finding further suggested that axitinib with different drug sensitivity profiles from current treatments of GIST could provide a new option for the clinic.

However, like sunitinib and regorafenib, axitinib still lacks high potency against the imatinib-resistant mutants occurring in the cKIT activation loop. As it is difficult to predict the conformational change of the activation loop mutations, which makes the rational design of new inhibitors very challenging, drug repurposing strategies might still be a feasible approach to find drugs to overcome these mutations.

Funding

This work was supported by the National Natural Science Foundation of China (grant numbers 81703007, 81872748, 81673469, and 81773777), the ‘Personalized Medicines-Molecular Signature-Based Drug Discovery and Development’ Strategic Priority Research Program of the Chinese Academy of Sciences (grant number XDA12020224), the Natural Science Foundation of Anhui Province (grant numbers 1808085QH263 and 1808085MH268), the Key Research and Development Program of Anhui Province (grant

number 1704a0802140), the China Postdoctoral Science Foundation (grant numbers 2018T110633 and 2017M612103), the Presidential Foundation of Hefei Institutes of Physical Science of CAS (grant number YZJJ2018QN17), and the Frontier Science Key Research Program of CAS (grant number QYZDB-SSW-SLH037). We are also grateful for the National Program for Support of Top-Notch Young Professionals for JL and the support of Hefei leading talent for FZ.

Conflict of interest statement

The authors declare that there are no conflicts of interest.

Supplemental material

Supplemental material for this article is available online.

ORCID iD

Jing Liu  <https://orcid.org/0000-0001-9513-3591>

References

- Hirota S, Isozaki K, Moriyama Y, *et al.* Gain-of-function mutations of c-kit in human gastrointestinal stromal tumors. *Science* 1998; 279: 577–580.
- Duensing A, Medeiros F, McConarty B, *et al.* Mechanisms of oncogenic KIT signal transduction in primary gastrointestinal stromal tumors (GISTs). *Oncogene* 2004; 23: 3999–4006.
- Rubin BP, Singer S, Tsao C, *et al.* KIT activation is a ubiquitous feature of gastrointestinal stromal tumors. *Cancer Res* 2001; 61: 8118–8121.
- Mei L, Smith SC, Faber AC, *et al.* Gastrointestinal stromal tumors: the GIST of precision medicine. *Trends Cancer* 2018; 4: 74–91.
- Corless CL, Barnett CM and Heinrich MC. Gastrointestinal stromal tumours: origin and molecular oncology. *Nat Rev Cancer* 2011; 11: 865–878.
- Neuhann TM, Mansmann V, Merkelbach-Bruse S, *et al.* A novel germline KIT mutation (p.L576P) in a family presenting with juvenile onset of multiple gastrointestinal stromal tumors, skin hyperpigmentations, and esophageal stenosis. *Am J Surg Pathol* 2013; 37: 898–905.
- Emile JF, Brahimi S, Coindre JM, *et al.* Frequencies of KIT and PDGFRA mutations in the MolecGIST prospective population-based study differ from those of advanced GISTs. *Med Oncol* 2012; 29: 1765–1772.
- Chen LL, Trent JC, Wu EF, *et al.* A missense mutation in KIT kinase domain 1 correlates with imatinib resistance in gastrointestinal stromal tumors. *Cancer Res* 2004; 64: 5913–5919.
- Wardelmann E, Merkelbach-Bruse S, Pauls K, *et al.* Polyclonal evolution of multiple secondary KIT mutations in gastrointestinal stromal tumors under treatment with imatinib mesylate. *Clin Cancer Res* 2006; 12: 1743–1749.
- Tutone M, Lauria A and Almerico AM. Study of the role of “gatekeeper” mutations V654A and T670I of c-kit kinase in the interaction with inhibitors by means mixed molecular dynamics/docking approach. *Bioinformation* 2011; 7: 296–298.
- Tuveson DA, Willis NA, Jacks T, *et al.* STI571 inactivation of the gastrointestinal stromal tumor c-KIT oncoprotein: biological and clinical implications. *Oncogene* 2001; 20: 5054–5058.
- Demetri GD, von Mehren M, Blanke CD, *et al.* Efficacy and safety of imatinib mesylate in advanced gastrointestinal stromal tumors. *N Engl J Med* 2002; 347: 472–480.
- Heinrich MC, Maki RG, Corless CL, *et al.* Primary and secondary kinase genotypes correlate with the biological and clinical activity of sunitinib in imatinib-resistant gastrointestinal stromal tumor. *J Clin Oncol* 2008; 26: 5352–5359.
- Nishida T, Takahashi T, Nishitani A, *et al.* Sunitinib-resistant gastrointestinal stromal tumors harbor cis-mutations in the activation loop of the KIT gene. *Int J Clin Oncol* 2009; 14: 143–149.
- Demetri GD, van Oosterom AT, Garrett CR, *et al.* Efficacy and safety of sunitinib in patients with advanced gastrointestinal stromal tumour after failure of imatinib: a randomised controlled trial. *Lancet* 2006; 368: 1329–1338.
- Demetri GD, Reichardt P, Kang YK, *et al.* Efficacy and safety of regorafenib for advanced gastrointestinal stromal tumours after failure of imatinib and sunitinib (GRID): an international, multicentre, randomised, placebo-controlled, phase 3 trial. *Lancet* 2013; 381: 295–302.
- Heinrich MC, Maki RG, Corless CL, *et al.* Primary and secondary kinase genotypes correlate with the biological and clinical activity of sunitinib in imatinib-resistant gastrointestinal stromal tumor. *J Clin Oncol* 2008; 26: 5352–5359.
- Garner AP, Gozgit JM, Anjum R, *et al.* Ponatinib inhibits polyclonal drug-resistant KIT

- oncoproteins and shows therapeutic potential in heavily pretreated gastrointestinal stromal tumor (GIST) patients. *Clin Cancer Res* 2014; 20: 5745–5755.
19. Massaro F, Molica M and Breccia M. Ponatinib: a review of efficacy and safety. *Curr Cancer Drug Targets*. 2017. DOI: 10.2174/1568009617666171002142659.
 20. Richters A, Ketzer J, Getlik M, *et al.* Targeting gain of function and resistance mutations in Abl and KIT by hybrid compound design. *J Med Chem* 2013; 56: 5757–5772.
 21. Worlein JM, Baker K, Bloomsmith M, *et al.* The eighth edition of the guide for the care and use of laboratory animals (2011); implications for behavioral management. *Am J Primatol* 2011; 73: 98.
 22. Liu X, Krawczyk E, Suprynowicz FA, *et al.* Conditional reprogramming and long-term expansion of normal and tumor cells from human biospecimens. *Nat Protoc* 2017; 12: 439–451.
 23. Roberts KG, Odell AF, Byrnes EM, *et al.* Resistance to c-KIT kinase inhibitors conferred by V654A mutation. *Mol Cancer Ther* 2007; 6: 1159–1166.
 24. Davis MI, Hunt JP, Herrgard S, *et al.* Comprehensive analysis of kinase inhibitor selectivity. *Nature Biotechnol* 2011; 29: 1046–1051.
 25. Fu J, Bian M, Jiang Q, *et al.* Roles of Aurora kinases in mitosis and tumorigenesis. *Mol Cancer Res* 2007; 5: 1–10.
 26. Crosio C, Fimia GM, Loury R, *et al.* Mitotic phosphorylation of histone H3: spatio-temporal regulation by mammalian Aurora kinases. *Mol Cell Biol* 2002; 22: 874–885.
 27. Harrington EA, Bebbington D, Moore J, *et al.* VX-680, a potent and selective small-molecule inhibitor of the Aurora kinases, suppresses tumor growth in vivo. *Nat Med* 2004; 10: 262–267.
 28. Qi W, Spier C, Liu X, *et al.* Alisertib (MLN8237) an investigational agent suppresses Aurora A and B activity, inhibits proliferation, promotes endoreduplication and induces apoptosis in T-NHL cell lines supporting its importance in PTCL treatment. *Leuk Res* 2013; 37: 434–439.
 29. Koumariou A, Economopoulou P, Katsaounis P, *et al.* Gastrointestinal stromal tumors (GIST): a prospective analysis and an update on biomarkers and current treatment concepts. *Biomark Cancer* 2015; 7: 1–7.
 30. Rugo HS, Herbst RS, Liu G, *et al.* Phase I trial of the oral antiangiogenesis agent AG-013736 in patients with advanced solid tumors: pharmacokinetic and clinical results. *J Clin Oncol* 2005; 23: 5474–5483.
 31. Abrams T, Connor A, Fanton C, *et al.* Preclinical antitumor activity of a novel anti-c-KIT antibody-drug conjugate against mutant and wild-type c-KIT-positive solid tumors. *Clin Cancer Res* 2018; 24: 4297–4308.
 32. Janeway KA, Kim SY, Lodish M, *et al.* Defects in succinate dehydrogenase in gastrointestinal stromal tumors lacking KIT and PDGFRA mutations. *P Natl Acad Sci USA* 2011; 108: 314–318.
 33. Janeway KA and Pappo A. Treatment guidelines for gastrointestinal stromal tumors in children and young adults. *J Pediat Hematol Onc* 2012; 34: S69–S72.

Visit SAGE journals online
journals.sagepub.com/
home/tam

 SAGE journals